Published in final edited form as:

J Am Coll Cardiol. 2021 October 05; 78(14): 1437–1449. doi:10.1016/j.jacc.2021.07.056.

Hepatic Sensing Loop Regulates PCSK9 Secretion in Response to Inhibitory Antibodies

Carlota Oleaga, PHD[a], **Michael D. Shapiro, MD**[a], **Joshua Hay, MS**[a], **Paul A. Mueller, PHD**[a], **Joshua Miles, MS**[a], **Cecilia Huang, MD**[a], **Emily Friz, BS**[a], **Hagai Tavori, PHD**[a], **Peter P. Toth, MD, PHD**[b,c], **Cezary Wójcik, MD, PHD, DS**[a], **Bruce A. Warden, PHARMD**[a], **Jonathan Q. Purnell, MD**[a], **P. Barton Duell, MD**[a], **Nathalie Pamir, PHD**[a], **Sergio Fazio, MD, PHD**[a]

[a]Knight Cardiovascular Institute, Center for Preventive Cardiology, Oregon Health and Science University, Portland, Oregon, USA

[b]Ciccarone Center for the Prevention of Cardiovascular Disease, Johns Hopkins University, and School of Medicine, Baltimore, Maryland, USA

[c]CGH Medical Center, Sterling, Illinois, USA.

Abstract

BACKGROUND—Monoclonal antibodies against proprotein convertase subtilisin/kexin type 9 (PCSK9i) lower LDL-C by up to 60% and increase plasma proprotein convertase subtilisin/kexin type 9 (PCSK9) levels by 10-fold.

OBJECTIVES—The authors studied the reasons behind the robust increase in plasma PCSK9 levels by testing the hypothesis that mechanisms beyond clearance via the low-density lipoprotein receptor (LDLR) contribute to the regulation of cholesterol homeostasis.

METHODS—In clinical cohorts, animal models, and cell-based studies, we measured kinetic changes in PCSK9 production and clearance in response to PCSK9i.

RESULTS—In a patient cohort receiving PCSK9i therapy, plasma PCSK9 levels rose 11-fold during the first 3 months and then plateaued for 15 months. In a cohort of healthy volunteers, a single injection of PCSK9i increased plasma PCSK9 levels within 12 hours; the rise continued for 9 days until it plateaued at 10-fold above baseline. We recapitulated the rapid rise in PCSK9 levels in a mouse model, but only in the presence of LDLR. In vivo turnover and in vitro pulse-chase studies identified 2 mechanisms contributing to the rapid increase in plasma PCSK9 levels in response to PCSK9i: 1) the expected delayed clearance of the antibody-bound PCSK9; and 2) the unexpected post-translational increase in PCSK9 secretion.

ADDRESS FOR CORRESPONDENCE: Dr Nathalie Pamir, Knight Cardiovascular Institute, Center for Preventive Cardiology, Oregon Health and Science University, 3161 SW Pavilion Loop, Mail Code UHN62, Portland, Oregon 97239, USA, pamir@ohsu.edu. Twitter: @pamirlab, @OHSUCardio.

The authors attest they are in compliance with human studies committees and animal welfare regulations of the authors' institutions and Food and Drug Administration guidelines, including patient consent where appropriate. For more information, visit the Author Center.

APPENDIX For an expanded Methods section as well as supplemental figures and tables, please see the online version of this paper.

CONCLUSIONS—PCSK9 re-entry to the liver via LDLR triggers a sensing loop regulating PCSK9 secretion. PCSK9i therapy enhances the secretion of PCSK9, an effect that contributes to the increased plasma PCSK9 levels in treated subjects.

Keywords

cholesterol homeostasis; LDL cholesterol; LDL receptor; monoclonal antibodies; PCSK9; turnover studies

Proprotein convertase subtilisin/kexin type 9 (PCSK9) is a low-abundance circulatory protein that binds to and induces the degradation of the low-density lipoprotein receptor (LDLR) (1,2), thus contributing to elevated low-density lipoprotein cholesterol (LDL-C) levels in plasma (3–6). Current understanding of PCSK9 biology is insufficient to explain how PCSK9—a low-abundance protein—can saturate and degrade a high-abundance protein, hepatic LDLR.

The discovery of PCSK9 in 2003 revolutionized our understanding of body cholesterol metabolism. Just 12 years later, monoclonal antibodies that block PCSK9 function entered the market (7). Monoclonal antibodies bind to plasma PCSK9, prevent LDLR-PCSK9 binding, and dramatically increase LDLR density on the liver cell surface. As a result, plasma LDL-C concentrations drop by an average of 50%−60% in patients with both inherited and acquired hypercholesterolemia (8,9). These monoclonal antibodies cause an extreme rise in total plasma PCSK9 levels (~10-fold on average) (10–14). Although the reduced LDLR-mediated PCSK9 clearance is undoubtedly a contributor, it is insufficient to explain the disproportionate rise in plasma PCSK9 levels. The limited understanding of the biochemical response to therapeutic PCSK9 reflects a limited understanding of basic PCSK9 biology, including regulation of secretion and turnover.

We characterized changes in plasma PCSK9, and lipid levels in a cohort of patients receiving PCSK9 inhibitors followed up to 18 months. We studied the mechanisms inducing plasma PCSK9 levels using an in vitro cell culture system, murine models with and without LDLR, and a cohort of healthy human volunteers. We show that the rise in plasma PCSK9 levels is a consequence of 2 kinetic changes, the expected reduced clearance caused by the interruption of LDLR-mediated pathway, and an unexpected and biologically significant increase in the secretion of preformed PCSK9. The latter observation suggests the presence of a hepatic sensing loop for internalized plasma PCSK9 blocked by the therapeutic antibodies.

METHODS

STUDY DESIGN.

We evaluated a patient cohort treated with proprotein convertase subtilisin/kexin type 9 inhibitory therapy with monoclonal antibodies (PCSK9i) under usual care management and measured lipid fractions and PCSK9 plasma levels over 18 months to assess the kinetics of the dramatic rise in plasma PCSK9 levels over time. We then set out to elucidate further the mechanism by which PCSK9 antibody therapy induces such a response, and studied the effect of PCSK9i in a group of healthy volunteers, in mice, and in an in vitro system.

THERAPEUTIC MONOCLONAL ANTIBODIES INHIBITING PCSK9 ACTION.

Therapeutic PCSK9i is detailed in the Supplemental Methods.

HUMAN STUDY SUBJECTS.

Human studies were approved by the Institutional Review Board of Oregon Health and Science University (#STUDY00017329 and #STUDY00020037). All participants signed the Institutional Review Board–approved informed consent.

Human cohort 1.—The first study group was prospectively enrolled in a clinical registry of PCSK9i users and retrospectively analyzed. Human plasma samples from a cohort of patients on PCSK9 inhibitory therapy were selected from our biorepository (15). Blood samples were collected under fasting conditions. Plasma lipid and PCSK9 levels from 172 hypercholesterolemic subjects at baseline and for up to 18 months on PCSK9i therapy were analyzed (Figure 1A). Table 1 includes the following patient demographics: prevalence of the clinical phenotype of familial hypercholesterolemia; plasma PCSK9 and lipid levels at baseline; and pharmacological therapy including lipid-lowering agents. We applied the American Heart Association criteria (16) or Dutch Lipid Clinic Network Score to identify familial hypercholesterolemia (FH).

Human cohort 2.—We studied kinetic changes from a single dose of PCSK9i (Figure 2A) in a cohort of 7 young and healthy volunteers. The study was approved by the OHSU IRB (#STUDY00020037). Table 2 describes the volunteer demographics: plasma PCSK9 and lipid levels at baseline, and type of PCSK9i.

Further details on human cohorts and plasma analysis are included in the Supplemental Methods.

ANIMAL STUDIES.

Animal experiments were carried out in compliance with National Institutes of Health guidelines and were approved by the Institutional Animal Care and Use Committee of Oregon Health and Science University (IACUC# IP00000744 and IP00002733). Eight-week-old C57BL/6 wild-type (WT) and LDLR knockout ($Ldlr^{-/-}$) mice were purchased (Cat# 000664 and 002207, respectively) from Jackson Laboratories. Two groups of mice were used in this the study, and details are given in the Supplemental Methods.

IN VITRO CELLULAR STUDIES.

Human embryonic kidney HEK293T cells (Cat# CRL-1573, ATCC) were grown as previously described (3,5) at 37 °C in a 5% CO_2 humidified atmosphere and transfected following our previously published protocol (17). Media formulations and experimental methodology (*Pulse-chase studies*) are detailed in the Supplemental Methods.

STATISTICS.

All relevant values are expressed as mean ± SE. All statistical analyses were run either in Microsoft Excel or Prism 8.3 (GraphPad Software, LLC). The threshold for statistical significance was defined as a P value <0.05. Statistical analyses included unpaired Student's

t-test, 1-way analysis of variance, linear mixed-effects model followed by Dunnet's post hoc comparative analysis, 2-way analysis of variance, and 1-phase nonlinear decay regression.

RESULTS

PLASMA PCSK9 LEVELS INCREASE THE FIRST 3 MONTHS OF THERAPY AND REMAIN ELEVATED THROUGHOUT THE 18-MONTH TREATMENT PERIOD.

We evaluated changes in plasma lipids and PCSK9 levels in a cohort of hypercholesterolemic patients (Human Cohort 1) treated with either evolocumab (140 mg biweekly, n = 113) or alirocumab (75 mg biweekly, n = 59) for 18 months (Figure 1A, Supplemental Figure 1) (see also the Methods section and Table 1).

LDL-C levels were reduced by 54 ± 2% ($P < 0.001$) within the first 3 months and then remained unchanged for the rest of the study period, in agreement with the efficacy of PCSK9i reported in clinical trials (Figures 1B and 1D). Similarly, changes in other lipid levels occurred within the first 3 months of therapy and remained stable thereafter; total cholesterol decreased 34 ± 2% ($P < 0.001$) (Supplemental Figures 1A and 1B); HDL-C increased 7 ± 3% ($P < 0.001$) (Supplemental Figures 1C and 1D); triglycerides decreased 18 ± 5% ($P < 0.001$) (Supplemental Figures 1E and 1F); and very low-density lipoprotein cholesterol decreased 18 ± 4% ($P < 0.001$) (Supplemental Figures 1G and 1H).

PCSK9i treatment induced an average 11-fold increase in plasma PCSK9 levels ($P < 0.001$) within the first 3 months, and levels stayed elevated for the remaining study period (10 ± 0.3-fold; $P < 0.001$) (Figures 1C and 1E).

To understand the timeline of long-term PCSK9 elevation on inhibitory therapy, we quantified changes in PCSK9 levels at 3, 12, 24, 72, 216, and 504 hours after a single administration of PCSK9i in a cohort of healthy volunteers (Human Cohort 2; evolocumab 140 mg, n = 4; alirocumab 75 mg, n = 3) (see also the Methods section, Table 2, and Figure 2A).

Plasma PCSK9 levels increased 1.7 ± 0.19-fold ($P < 0.05$) within 12 hours after injection and continued to grow daily, reaching a maximum of 10.4 ± 1.6-fold ($P < 0.001$) at day 9 ($P < 0.001$) (Figures 2B and 2D). LDL-C levels started decreasing by the third day (11 ± 3%; $P < 0.01$) and reached the maximum decrease (40 ± 3%; $P < 0.01$) by the 21st day ($P < 0.001$) (Figures 2C and 2E). Plasma total cholesterol levels were moderately reduced ($P < 0.01$) (Supplemental Figure 2B and 2D), whereas HDL-C levels were unaffected during this study (Supplemental Figures 2C and 2E).

We quantified changes in plasma PCSK9 levels after a single administration of PCSK9i in WT and LDLR deficient mice ($Ldlr^{-/-}$) (Murine Cohort 1) (Figure 3A). In PCSK9i-treated WT mice, plasma PCSK9 levels increased 7 ± 2-fold ($P < 0.01$) from baseline within 2 hours from injection and continued to rise for 16 hours, with a cumulative increase of 21 ± 4-fold ($P < 0.001$) (Figure 3B). Return to physiological PCSK9 levels occurred 2 weeks after the single injection (Supplemental Figure 3). As expected, $Ldlr^{-/-}$ mice had 16 times greater baseline plasma PCSK9 levels when compared with WT mice caused by the lack of

LDLR-mediated clearance of PCSK9 (1,069 ± 95 ng/mL vs 67 ± 10 ng/mL, respectively; $P < 0.001$). The administration of PCSK9i in $Ldlr^{-/-}$ mice failed to increase plasma PCSK9 levels (Figure 3C).

PCSK9i DELAYS PCSK9 CLEARANCE.

Because PCSK9i therapy blocks the interaction between PCSK9 and LDLR, and LDLR is the main clearance pathway for PCSK9, we tested the hypothesis that the interrupted clearance is the exclusive reason for the rise in PCSK9 levels in response to PCSK9i. In WT mice (Murine Cohort 2) (Figure 4A), PCSK9 bound to a monoclonal antibody had a half-life which was more than double that of unbound PCSK9 (34 minutes vs 14 minutes; $P < 0.01$) (Figure 4B). Consistent with the previous mouse kinetic experiments (Figure 3), endogenous plasma PCSK9 levels increased as early as 1 hour after PCSK9i injection (2 ± 0.3-fold; $P < 0.05$) (Figure 4C), and continued to increase for the duration of the study ($P < 0.001$).

PCSK9 BLOCKADE ASSOCIATES WITH INCREASED HEPATIC LDLR AND PCSK9 PROTEIN LEVELS AND WITH INCREASED PCSK9 SECRETION.

We quantified hepatic PCSK9 and LDLR protein levels after a single administration of PCSK9i in WT and $Ldlr^{-/-}$ mice (Murine Cohort 1) (Figure 5A). After 24 hours, livers of PCSK9i-treated WT mice expressed 2 ± 0.2-fold ($P < 0.001$) more LDLR protein than did vehicle-treated mice (Figure 5B); *Ldlr* mRNA levels were comparable between groups (Figure 5C). PCSK9i also induced a 27 ± 10% increase ($P = 0.0507$) in hepatic PCSK9 protein levels in WT mice (Figure 5D) without changing its gene expression (Figure 5E). PCSK9i administration in $Ldlr^{-/-}$ mice did not alter hepatic PCSK9 protein levels compared with control subjects (Figures 5D and 5E).

We evaluated PCSK9 synthesis and secretion kinetics in response to PCSK9i with a series of pulse-chase experiments in a PCSK9-expressing HEK cell model treated with either 8 μg/mL evolocumab or vehicle for 24 hours. We chose a renal cell line rather than a hepatocyte model because it allowed us to optimize the pulse-chase conditions. High transfection efficiency of HEK293T cells leads to intracellular (2.5-fold) and extracellular (16-fold) concentrations of PCSK9 much higher than achievable with HepG2 cells (17). In addition, HEK293T cells do not express endogenous PCSK9, thus serving as an excellent negative control for the immunoprecipitation studies (cells transfected with the empty vector: lanes 1 and 12 of pulse-chase gel images in Figures 6A and 6B). PCSK9 secretion gradually increased over time and was on average 2.1 ± 0.3-fold greater in PCSK9i treated cells than control subjects ($P < 0.05$), whereas synthesis of PCSK9 was unaffected (Figures 6A and 6B).

DISCUSSION

The fast progress from the discovery of PCSK9 to effective therapy to antagonize its effect is a testimony to the power of genetics leveraged to inform drug discovery. However, this rapid development means that gaps in knowledge relating to fundamental PCSK9 physiology remain. Here, we sought to reconcile the observation that PCSK9i therapy is associated with dramatic elevations in plasma PCSK9 concentration—an effect that appears to be too

large to be solely caused by impaired LDLR-dependent clearance. We characterized plasma PCSK9 and lipid levels in a cohort of patients undergoing PCSK9i therapy to understand kinetic changes induced by PCSK9 blockade. Plasma LDL-C decreased by ~60% and plasma PCSK9 levels increased by ~10-fold within 3 months of therapy initiation, consistent with previous reports (18,19). To understand the mechanism by which plasma PCSK9 increases after administration of PCSK9i, we investigated the time course of early response after a single dose of PCSK9i in healthy volunteers. We observed an unexpectedly rapid and steady increase in plasma PCSK9 levels starting at 12 hours and continuing for 9 days. On the other hand, PCSK9i-dependent changes in plasma lipid levels occurred more slowly and were asynchronous with the marked increase in plasma PCSK9. We confirmed these results in a murine model, where we observed a rapid and significant elevation in PCSK9 in response to PCSK9i that was LDLR-dependent. We showed that the PCSK9-antibody complex delays plasma PCSK9 clearance, increasing the half-life 2-fold, and determined that the blocked return of PCSK9 to the liver stimulates PCSK9 secretion via activation of a post-translational sensing mechanism (Central Illustration).

Previous studies with therapeutic monoclonal antibodies blocking tumor necrosis factor alpha have also reported an increase in plasma tumor necrosis factor alpha levels caused by its prolonged half-life (20–25). Circulating antibody-target complexes follow clearance pathways that are either dependent or independent from the target (26,27). PCSK9 is cleared from circulation mainly through the LDLR, although poorly defined LDLR-independent pathways are also likely involved (5,28–32). Antibody blockade of PCSK9 prolongs its plasma half-life, which undoubtedly contributes to the rise in circulating PCSK9 levels. Because monoclonal antibodies against PCSK9 limit LDLR dependent clearance of the PCSK9i-PCSK9 complex, pathways other than LDLR should be at play. In humans and WT mice, the rise in circulating PCSK9 induced by PCSK9i peaked within days after injection and then stabilized. In mice lacking LDLR—who already have high plasma PCSK9 levels because of impaired clearance (3–6,33)—PCSK9i did not influence plasma PCSK9 levels. Therefore, when the LDLR pathway is inaccessible to PCSK9 caused by LDLR deficiency or monoclonal antibody blockade, plasma PCSK9 levels will rise until they reach a threshold that triggers clearance of PCSK9 via an LDLR-independent pathway (5,28–32).

Although we confirmed that PCSK9 bound to its antibody had delayed plasma clearance, we questioned if this was the mechanism responsible for the rapid and drastic rise in plasma PCSK9 upon PCSK9i treatment. Transcription of PCSK9 is regulated by sterol regulatory element-binding proteins (SREBPs) and is increased by statin treatment (34,35). One could hypothesize that PCSK9i-induced preservation of hepatic LDLR causes intracellular cholesterol saturation and down-regulation of cholesterol synthesis via SREBP regulation (36–38). We searched for hepatic transcriptional up-regulation of PCSK9 triggered by a feedback response from antibody blockade, but determined that PCSK9i did not affect hepatic PCSK9 synthesis.

We focused on the possibility of changes in secretory activity of PCSK9 after identifying a small but significant increase in hepatic PCSK9 protein levels in the mouse experiments. Our pulse-chase studies demonstrate that PCSK9i significantly increases cellular secretion of PCSK9 without affecting hepatic PCSK9 synthesis. Increased secretion may result from

changes in the stability or compartmentalization of intracellular PCSK9 (39). Even though the ultimate mechanism has yet to be elucidated, our results suggest that a post-translational cellular sensing mechanism regulates PCSK9 secretion perhaps more significantly than the transcriptional control exerted by SREBP. Spolitu et al (40), found that glucagon down-regulates PCSK9 post-transcriptionally, reducing the stability of intracellular PCSK9, and this translates in reduced secretion of PCSK9. It is plausible to envision that the liver cell senses the number of PCSK9 molecules returning from the circulation and uses this information to regulate the secretion of new PCSK9 accordingly, as seen in other cell types for hormones, neurotransmitters, and other secretory proteins under feedback loop regulation (41). Considering that plasma PCSK9 has a fractional catabolic rate of 2 pools/d (42–45) that PCSK9i reduces clearance of injected PCSK9 in mice by 41% (Figure 4), we extrapolated these data to the human model (Figure 2) to estimate that impaired clearance contributes 72% of the total PCSK9 increase, with the remaining 28% caused by increased secretion. Future studies of hepatic RNAseq before and after PCSK9 inhibitor may identify gene networks that contribute to the regulation of PCSK9 secretion.

PCSK9 binding to the LDLR is abolished both in cell-free and cell-based assays by antibodies targeting PCSK9 (46). Disruption of PCSK9-LDLR interaction is still compatible with downstream signaling effects, as the antibody-antigen complex may still clear the circulation and enter the liver via LDLR-independent target-mediated mechanisms. For example, we have shown that plasma PAI-1 levels decrease following PCSK9 blockade, an effect that most probably is independent of LDLR (47). However, no metabolic effects of the increased plasma PCSK9 levels induced by PCSK9i therapy have been thus far identified, although we can speculate that situations leading to dissociation of the antigen from the therapeutic antibody would likely trigger an increase in cholesterol levels. One such situation is when the antibody is discontinued, and thus, newly secreted PCSK9 will be again free to act on the LDLR and additional PCSK9 is released by the immune complex (by virtue of the law of mass action), because the dissociation rate will exceed the association rate caused by the diminishing antibody concentration (48). Likewise, the increased PCSK9 secretion induced by antibody blockade, if it persists after discontinuing the antibody, will drive cholesterol levels above baseline. It must be noted, though, that no animal or human studies thus far have reported the presence of a rebound in cholesterol levels after stopping the blocking antibody.

DATA AND STUDY LIMITATIONS.

We used a translational approach to decipher the kinetic changes induced in PCSK9 by the therapeutic blockade with monoclonal antibodies. This strategy is powerful and has allowed us to pinpoint the contributing mechanisms to the kinetic changes. Nevertheless, the results obtained in the different models (human, mice, and cells) cannot be extrapolated to calculate PCSK9 turnover because they differ in kinetic rates. Thus, we can only estimate the relative contribution of the 2 mechanisms described to the increase plasma PCSK9. Our pulse-chase experiments suggest that the cells can sense the return of circulating PCSK9 and regulate secretion of preformed PCSK9 accordingly. However, the in vitro system used in these experiments is based on kidney HEK293T cells, which were transfected to express PCSK9. These findings will need to be validated in in vivo systems

CONCLUSIONS

We determined that the rise in plasma PCSK9 levels induced by PCSK9i is explained by 2 mechanisms: 1) the expected decreased clearance of circulating PCSK9 caused by the blocked interaction with LDLR; and 2) an unexpected increased secretion of cellular PCSK9 in response to lack of re-entry of PCSK9 from plasma (Central Illustration). This novel cellular sensing mechanism may be of critical value in PCSK9 regulation, and suggests a plausible explanation for how a low-abundance protein like PCSK9 manages to regulate a high-abundance receptor like LDLR.

Supplementary Material

Refer to Web version on PubMed Central for supplementary material.

ACKNOWLEDGMENTS

The authors thank Tina Kaufman, physician assistant, for performing the subcutaneous injections of PCSK9i in the small human cohort; and all the volunteers of the study. The authors also thank Amgen for supplying the murine monoclonal antibody against murine PCSK9. Bio-render was used to create the cartoons.

FUNDING SUPPORT AND AUTHOR DISCLOSURES

This work was supported by the National Institutes of Health (5RO1HL132985). Dr Shapiro has received compensation for advisory activities from Amgen, Esperion, and Novartis. Dr Toth has served as a member of the Speakers Bureau for Amarin, Amgen, Esperion, and Novo Nordisk; and has served as a consultant to Amarin, 89bio, Kowa, Novartis, Resverlogix, and Theravance. Dr Wójcik is a current employee of Amgen; and has served as a consultant for Esperion and The Medicines Company. Dr Duell has performed advisory activities for Akcea, Amryt, Esperion, Kaneka, and Regeneron; and has received institutional grants from Retrophin/Travere, Regeneron, and Regenxbio. Dr Fazio is currently an employee of Regeneron Pharmaceuticals; during the covered period while at OHSU he received compensation for advisory activities from Amarin, Kowa, Novo Nordisk, Novartis, 89bio, and Esperion. All other authors have reported that they have no relationships relevant to the contents of this paper to disclose.

ABBREVIATIONS AND ACRONYMS

LDL-C	low-density lipoprotein cholesterol
LDLR	low-density lipoprotein receptor
Ldlr$^{-/-}$	low-density lipoprotein receptor deficient mice
PCSK9	proprotein convertase subtilisin/kexin type 9
PCSK9i	proprotein convertase subtilisin/kexin type 9 inhibitory therapy with monoclonal antibodies
SREBP	sterol regulatory element-binding protein
WT	wild type

REFERENCES

1. Abifadel M, Varret M, Rabes JP, et al. Mutations in PCSK9 cause autosomal dominant hypercholesterolemia. Nat Genet. 2003;34:154–156. [PubMed: 12730697]

2. Seidah NG, Benjannet S, Wickham L, et al. The secretory proprotein convertase neural apoptosis-regulated convertase 1 (NARC-1): liver regeneration and neuronal differentiation. Proc Natl Acad Sci U S A. 2003;100:928–933. [PubMed: 12552133]
3. Fan D, Yancey PG, Qiu S, et al. Self-association of human PCSK9 correlates with its LDLR-degrading activity. Biochemistry. 2008;47:1631–1639. [PubMed: 18197702]
4. Lagace TA. PCSK9 and LDLR degradation: regulatory mechanisms in circulation and in cells. Curr Opin Lipidol. 2014;25:387–393. [PubMed: 25110901]
5. Tavori H, Fan D, Blakemore JL, et al. Serum proprotein convertase subtilisin/kexin type 9 and cell surface low-density lipoprotein receptor: evidence for a reciprocal regulation. Circulation. 2013;127:2403–2413. [PubMed: 23690465]
6. Tavori H, Rashid S, Fazio S. On the function and homeostasis of PCSK9: reciprocal interaction with LDLR and additional lipid effects. Atherosclerosis. 2015;238:264–270. [PubMed: 25544176]
7. Seidah NG. The PCSK9 revolution and the potential of PCSK9-based therapies to reduce LDL-cholesterol. Glob Cardiol Sci Pract. 2017;2017: e201702. [PubMed: 28971102]
8. Sabatine MS, Giugliano RP, Keech AC, et al. Evolocumab and clinical outcomes in patients with cardiovascular disease. N Engl J Med. 2017;376: 1713–1722. [PubMed: 28304224]
9. Robinson JG, Farnier M, Kastelein JJP, et al. Relationship between alirocumab, PCSK9, and LDL-C levels in four phase 3 ODYSSEY trials using 75 and 150 mg doses. J Clin Lipidol. 2019;13:979–988.e10. [PubMed: 31708410]
10. Roth EM, McKenney JM, Hanotin C, Asset G, Stein EA. Atorvastatin with or without an antibody to PCSK9 in primary hypercholesterolemia. N Engl J Med. 2012;367:1891–1900. [PubMed: 23113833]
11. Koren MJ, Roth EM, McKenney JM, et al. Safety and efficacy of alirocumab 150 mg every 2 weeks, a fully human proprotein convertase subtilisin/kexin type 9 monoclonal antibody: A Phase II pooled analysis. Postgrad Med. 2015;127:125–132. [PubMed: 25609019]
12. Ridker PM, Tardif JC, Amarenco P, et al. Lipid-reduction variability and antidrug-antibody formation with bococizumab. N Engl J Med. 2017;376:1517–1526. [PubMed: 28304227]
13. Shapiro MD, Miles J, Tavori H, Fazio S. Diagnosing resistance to a proprotein convertase subtilisin/kexin type 9 inhibitor. Ann Intern Med. 2018;168:376–379. [PubMed: 29181527]
14. Zhang L, McCabe T, Condra JH, et al. An anti-PCSK9 antibody reduces LDL-cholesterol on top of a statin and suppresses hepatocyte SREBP-regulated genes. Int J Biol Sci. 2012;8:310–327. [PubMed: 22355267]
15. Kaufman TM, Duell PB, Purnell JQ, Wojcik C, Fazio S, Shapiro MD. Application of PCSK9 inhibitors in practice: challenges and opportunities. Circ Res. 2017;121:499–501. [PubMed: 28819040]
16. Gidding SS, Champagne MA, de Ferranti SD, et al. The agenda for familial hypercholesterolemia: a scientific statement from the American Heart Association. Circulation. 2015;132:2167–2192. [PubMed: 26510694]
17. Oleaga C, Hay J, Gurcan E, et al. Insights on the kinetics and dynamics of the furin-cleaved form of PCSK9. J Lipid Res. Published online November 23, 2020.10.1194/jlr.RA120000964
18. Watts GF, Chan DC, Dent R, et al. Factorial Effects of evolocumab and atorvastatin on lipoprotein metabolism. Circulation. 2017;135:338–351. [PubMed: 27941065]
19. Warden BA, Fazio S, Shapiro MD. The PCSK9 revolution: current status, controversies, and future directions. Trends Cardiovasc Med. 2020;30:179–185. [PubMed: 31151804]
20. Berkhout LC, l'Ami MJ, Ruwaard J, et al. Dynamics of circulating TNF during adalimumab treatment using a drug-tolerant TNF assay. Sci Transl Med. 2019;11(477):eaat3356. 10.1126/scitranslmed.aat3356 [PubMed: 30700574]
21. Berthold E, Mansson B, Gullstrand B, et al. Tumour necrosis factor-alpha/etanercept complexes in serum predict long-term efficacy of etanercept treatment in seronegative rheumatoid arthritis. Scand J Rheumatol. 2018;47:22–26. [PubMed: 28485187]
22. Charles P, Elliott MJ, Davis D, et al. Regulation of cytokines, cytokine inhibitors, and acute-phase proteins following anti-TNF-alpha therapy in rheumatoid arthritis. J Immunol. 1999;163:1521–1528. [PubMed: 10415055]

23. Cornillie F, Shealy D, D'Haens G, et al. Infliximab induces potent anti-inflammatory and local immunomodulatory activity but no systemic immune suppression in patients with Crohn's disease. Aliment Pharmacol Ther. 2001;15:463–473. [PubMed: 11284774]
24. Kahn R, Berthold E, Gullstrand B, et al. Circulating complexes between tumour necrosis factor-alpha and etanercept predict long-term efficacy of etanercept in juvenile idiopathic arthritis. Acta Paediatr. 2016;105:427–432. [PubMed: 26707699]
25. Schulz M, Dotzlaw H, Neeck G. Ankylosing spondylitis and rheumatoid arthritis: serum levels of TNF-alpha and its soluble receptors during the course of therapy with etanercept and infliximab. Biomed Res Int. 2014;2014:675108. [PubMed: 24783218]
26. Kasichayanula S, Grover A, Emery MG, et al. Clinical pharmacokinetics and pharmacodynamics of evolocumab, a PCSK9 inhibitor. Clin Pharmacokinet. 2018;57:769–779. [PubMed: 29353350]
27. Manniello M, Pisano M. Alirocumab (Praluent): first in the new class of PCSK9 inhibitors. P T. 2016;41:28–53. [PubMed: 26766888]
28. Cameron J, Bogsrud MP, Tveten K, et al. Serum levels of proprotein convertase subtilisin/kexin type 9 in subjects with familial hypercholesterolemia indicate that proprotein convertase subtilisin/kexin type 9 is cleared from plasma by low-density lipoprotein receptor-independent pathways. Transl Res. 2012;160:125–130. [PubMed: 22683370]
29. Galvan AM, Chorba JS. Cell-associated heparin-like molecules modulate the ability of LDL to regulate PCSK9 uptake. J Lipid Res. 2019;60: 71–84. [PubMed: 30463987]
30. Gustafsen C, Olsen D, Vilstrup J, et al. Heparan sulfate proteoglycans present PCSK9 to the LDL receptor. Nat Commun. 2017;8:503. [PubMed: 28894089]
31. Lagace TA, Curtis DE, Garuti R, et al. Secreted PCSK9 decreases the number of LDL receptors in hepatocytes and in livers of parabiotic mice. J Clin Invest. 2006;116:2995–3005. [PubMed: 17080197]
32. Susan-Resiga D, Girard E, Kiss RS, et al. The proprotein convertase subtilisin/kexin type 9-resistant R410S low density lipoprotein receptor mutation: a novel mechanism causing familial hypercholesterolemia. J Biol Chem. 2017;292:1573–1590. [PubMed: 27998977]
33. Horton JD, Cohen JC, Hobbs HH. PCSK9: a convertase that coordinates LDL catabolism. J Lipid Res. 2009;50(Suppl):S172–S177. [PubMed: 19020338]
34. Jeong HJ, Lee H-S, Kim K-S, Kim Y-K, Yoon D, Park SW. Sterol-dependent regulation of proprotein convertase subtilisin/kexin type 9 expression by sterol-regulatory element binding protein-2. J Lipid Res. 2008;49:399–409. [PubMed: 17921436]
35. Dong B, Wu M, Li H, et al. Strong induction of PCSK9 gene expression through HNF1alpha and SREBP2: mechanism for the resistance to LDL-cholesterol lowering effect of statins in dyslipidemic hamsters. J Lipid Res. 2010;51:1486–1495. [PubMed: 20048381]
36. Brown MS, Goldstein JL. The SREBP pathway: regulation of cholesterol metabolism by proteolysis of a membrane-bound transcription factor. Cell. 1997;89:331–340. [PubMed: 9150132]
37. DeBose-Boyd RA, Ye J. SREBPs in lipid metabolism, insulin signaling, and beyond. Trends Biochem Sci. 2018;43:358–368. [PubMed: 29500098]
38. Weber LW, Boll M, Stampfl A. Maintaining cholesterol homeostasis: sterol regulatory element-binding proteins. World J Gastroenterol. 2004;10:3081–3087. [PubMed: 15457548]
39. Gustafsen C, Kjolby M, Nyegaard M, et al. The hypercholesterolemia-risk gene SORT1 facilitates PCSK9 secretion. Cell Metab. 2014;19: 310–318. [PubMed: 24506872]
40. Spolitu S, Okamoto H, Dai W, et al. Hepatic glucagon signaling regulates PCSK9 and low-density lipoprotein cholesterol. Circ Res. 2019;124:38–51. [PubMed: 30582457]
41. Gerber SH, Sudhof TC. Molecular determinants of regulated exocytosis. Diabetes. 2002;51(Suppl 1):S3–S11. [PubMed: 11815450]
42. Gibbs JP, Doshi S, Kuchimanchi M, et al. Impact of target-mediated elimination on the dose and regimen of evolocumab, a human monoclonal antibody against proprotein convertase subtilisin/kexin type 9 (PCSK9). J Clin Pharmacol. 2017;57: 616–626. [PubMed: 27861991]
43. Lassman ME, McAvoy T, Lee AY, et al. Practical immunoaffinity-enrichment LC-MS for measuring protein kinetics of low-abundance proteins. Clin Chem. 2014;60:1217–1224. [PubMed: 24751376]

44. Millar JS, Reyes-Soffer G, Jumes P, et al. Anacetrapib lowers LDL by increasing ApoB clearance in mildly hypercholesterolemic subjects. J Clin Invest. 2015;125:2510–2522. [PubMed: 25961461]

45. Wang C, Zheng Q, Zhang M, Lu H. Lack of ethnic differences in the pharmacokinetics and pharmacodynamics of evolocumab between Caucasian and Asian populations. Br J Clin Pharmacol. 2019;85:114–125. [PubMed: 30225890]

46. Duff CJ, Scott MJ, Kirby IT, Hutchinson SE, Martin SL, Hooper NM. Antibody-mediated disruption of the interaction between PCSK9 and the low-density lipoprotein receptor. Biochem J. 2009;419:577–584. [PubMed: 19196236]

47. Levine JA, Oleaga C, Eren M, et al. Role of PAI-1 in hepatic steatosis and dyslipidemia. Sci Rep. 2021;11(1):430. [PubMed: 33432099]

48. Reverberi R, Reverberi L. Factors affecting the antigen-antibody reaction. Blood Transfus. 2007;5:227–240. [PubMed: 19204779]

PERSPECTIVES

COMPETENCY IN MEDICAL KNOWLEDGE:

In patients treated with PCSK9i medication, a rise in plasma PCSK9 concentration can be used to confirm adherence to treatment and identify nonresponders. Plasma PCSK9 levels are raised by monoclonal antibodies through mechanisms that involve both delayed clearance and increased hepatic secretion.

TRANSLATIONAL OUTLOOK:

Although re-entry of circulating PCSK9 represents a novel regulatory mechanism that increases PCSK9 secretion during treatment with PCSK9 inhibitors, further research is necessary to determine the effect of chronically elevated intracellular levels on health outcomes.

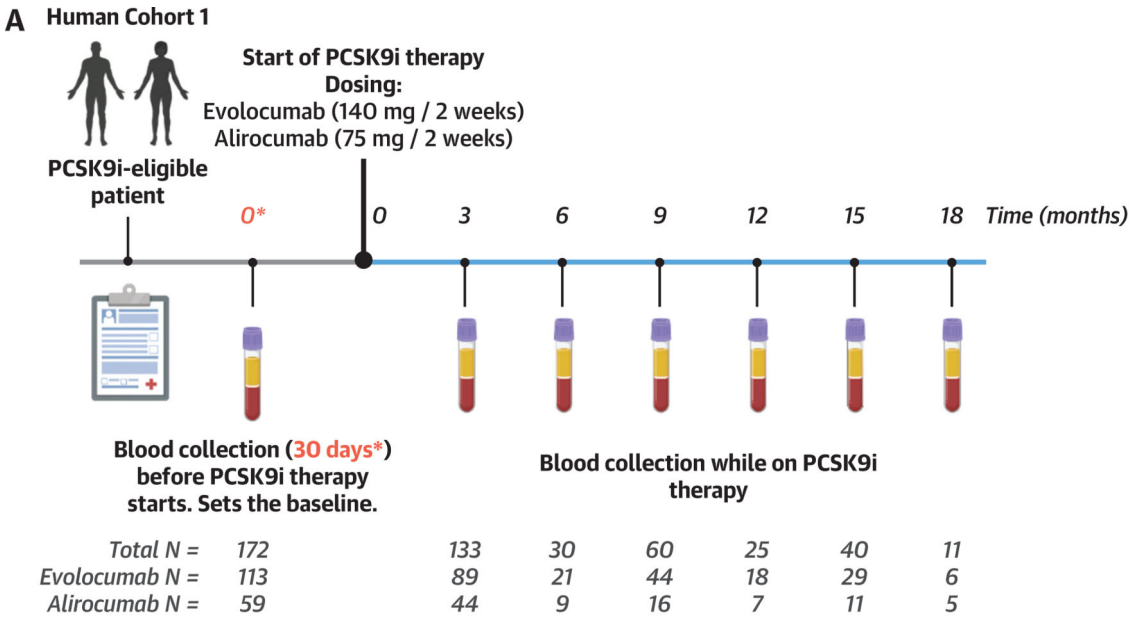

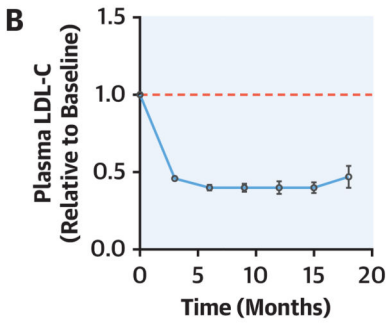

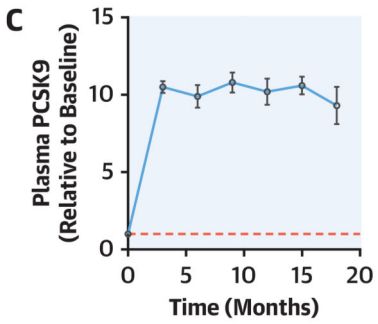

D

Plasma LDL-C (mg/dL)	Time (Months)						
	0	3	6	9	12	15	18
Mean ± SE	137 ± 4	64 ± 4	45 ± 4	52 ± 5	63 ± 8	55 ± 6	44 ± 6
95% CI	129-146	55-72	37-53	42-62	47-78	43-68	29-59

E

Plasma PCSK9 (ng/mL)	Time (Months)						
	0	3	6	9	12	15	18
Mean ± SE	400 ± 13	3,788 ± 129	3,639 ± 220	3,763 ± 175	3,687 ± 264	3,856 ± 244	3,602 ± 322
95% CI	374-427	3,532-4,044	3,189-4,090	3,412-4,113	3,142-4,232	3,362-4,349	2,899-4,304

FIGURE 1. Long-Term Effects of PCSK9i Therapy on Plasma PCSK9 and LDL-C Levels

Patients eligible for antibody-based proprotein convertase subtilisin/kexin type 9 (PCSK9) inhibition therapy received 140 mg evolocumab or 75 mg alirocumab every 2 weeks. Plasma was collected before initiation of therapy (time 0) and during the 18 months of treatment **(A)**. **(B and D)** Plasma LDL-C levels, and **(C and E)** plasma PCSK9 levels. Changes from baseline **(red dotted line)** are plotted (mean ± SE) **(B and C)** and absolute values are presented in the inset tables (mean ± SE, and 95% CI) **(D and E)**. Using absolute values, changes from baseline were analyzed by linear mixed-effects model ($P < 0.001$ for

PCSK9 and LDL-C) followed by Dunnet's post hoc test ($P < 0.001$ for all time points). CI = confidence interval; LDL-C = low-density lipoprotein cholesterol; PCSK9i = proprotein convertase subtilisin/kexin type 9 inhibitory therapy with monoclonal antibodies.

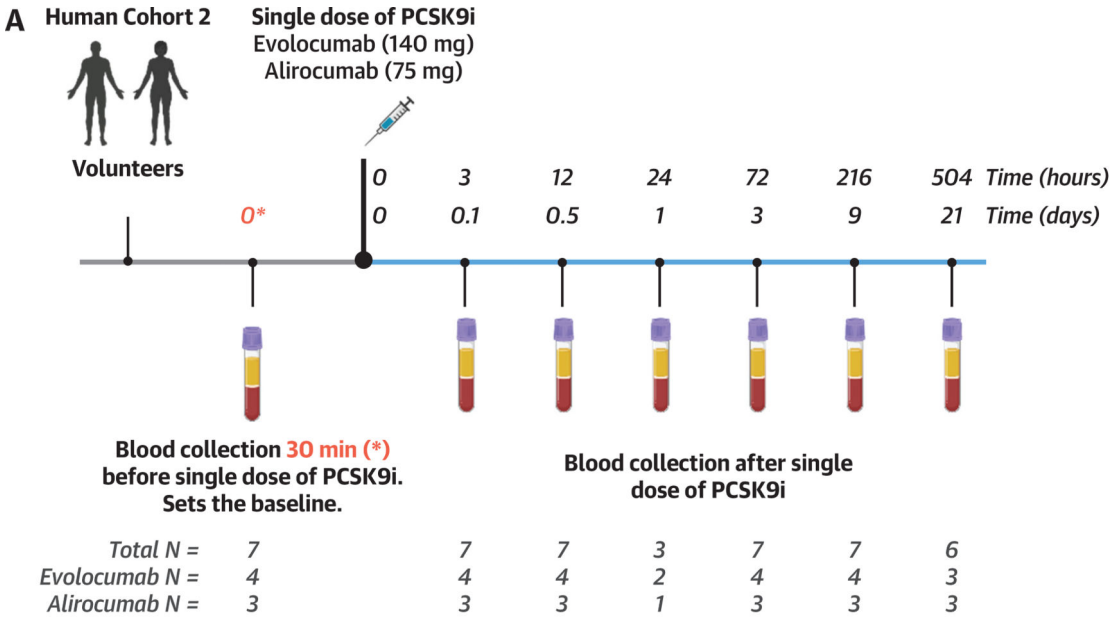

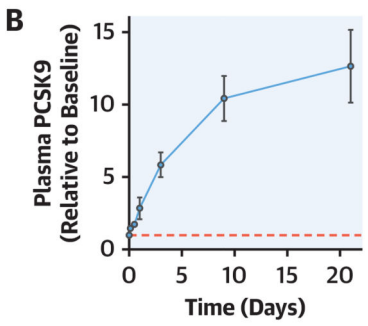

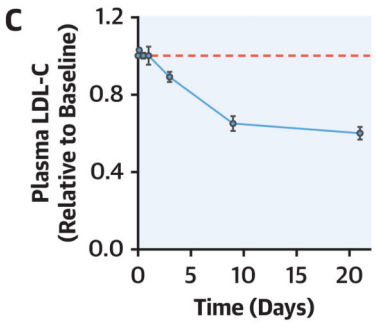

D

Plasma PCSK9 (ng/mL)	Time (Days)						
	0	0.1	0.5	1	3	9	21
Mean ± SE	214 ± 46	313 ± 78	343 ± 48	603 ± 110	1,100 ± 153	1,948 ± 200	1,944 ± 178
95% CI	191-370	122-503	225-461	130-1,076	726-1,474	1,460-2,436	1,487-2,400

E

Plasma LDL-C (mg/dL)	Time (Days)						
	0	0.1	0.5	1	3	9	21
Mean ± SE	104 ± 17	108 ± 14	103 ± 13	107 ± 113	92 ± 12	67 ± 10	64 ± 10
95% CI	75-131	75-140	72-135	54-161	63-120	43-92	39-89

FIGURE 2. Short-Term Response to PCSK9i in a Cohort of Healthy Volunteers

Participants received a single dose of either evolocumab (140 mg, n = 4) or alirocumab (75 mg, n = 3). Blood samples were collected 30 minutes prior to antibody injection, and then 3, 12, 24, 72, 216, and 504 hours after injection **(A)**. Plasma PCSK9 **(B and D)** and low-density lipoprotein cholesterol (LDL-C) **(C and E)** levels are presented as changes from baseline (mean ± SE) and absolute values are presented in the inset tables (mean ± SE, and 95% CI) **(D and E)**. Using absolute values, changes from baseline were analyzed by linear mixed-effects model ($P < 0.001$ for PCSK9 and LDL-C) followed by Dunnet's post hoc test

(PCSK9: 0.5 and 3–21 days; $P < 0.05$; LDL-C: 3–21 days; $P < 0.01$). Abbreviations as in Figure 1.

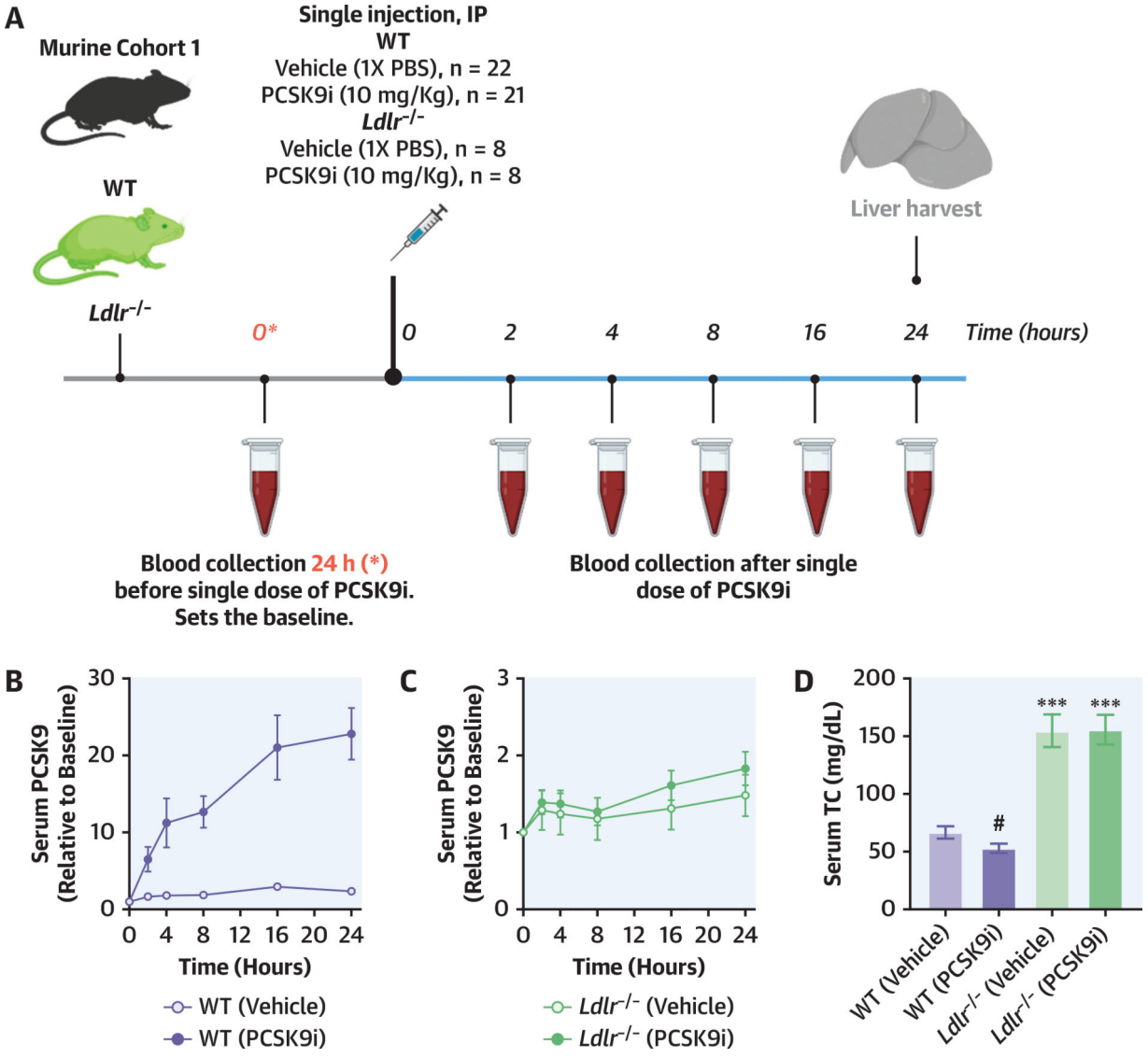

FIGURE 3. Short-Term Effects of PCSK9i in Mice

Wild type (WT) and low-density lipoprotein receptor deficient ($Ldlr^{-/-}$) mice were given a single peritoneal injection of PCSK9i antibody (10 mg/kg) or vehicle (phosphate-buffered saline [PBS]). Blood samples were collected 24 hours before injection, and then 2, 4, 8, 16, and 24 hours after injection **(A)**. PCSK9 plasma levels were quantified in WT **(B)** and $Ldlr^{-/-}$ **(C)** mice over time and plotted relative to baseline. Total cholesterol (TC) was quantified at the endpoint **(D)**. Values are mean ± SE (n = 6–22). Using absolute values, changes over time were analyzed by linear mixed-effects model ($P < 0.001$ for WT; $P > 0.05$ for $Ldlr^{-/-}$) followed by Dunnet's post hoc test (vehicle injected: all time points $P > 0.05$; PCSK9i injected: all time points; $P < 0.001$). Changes in total cholesterol were evaluated for significance by 2-tailed unpaired Student's *t*-test. #$P < 0.08$; ***$P < 0.001$. IP = intraperitoneal injections; other abbreviations as in Figure 1.

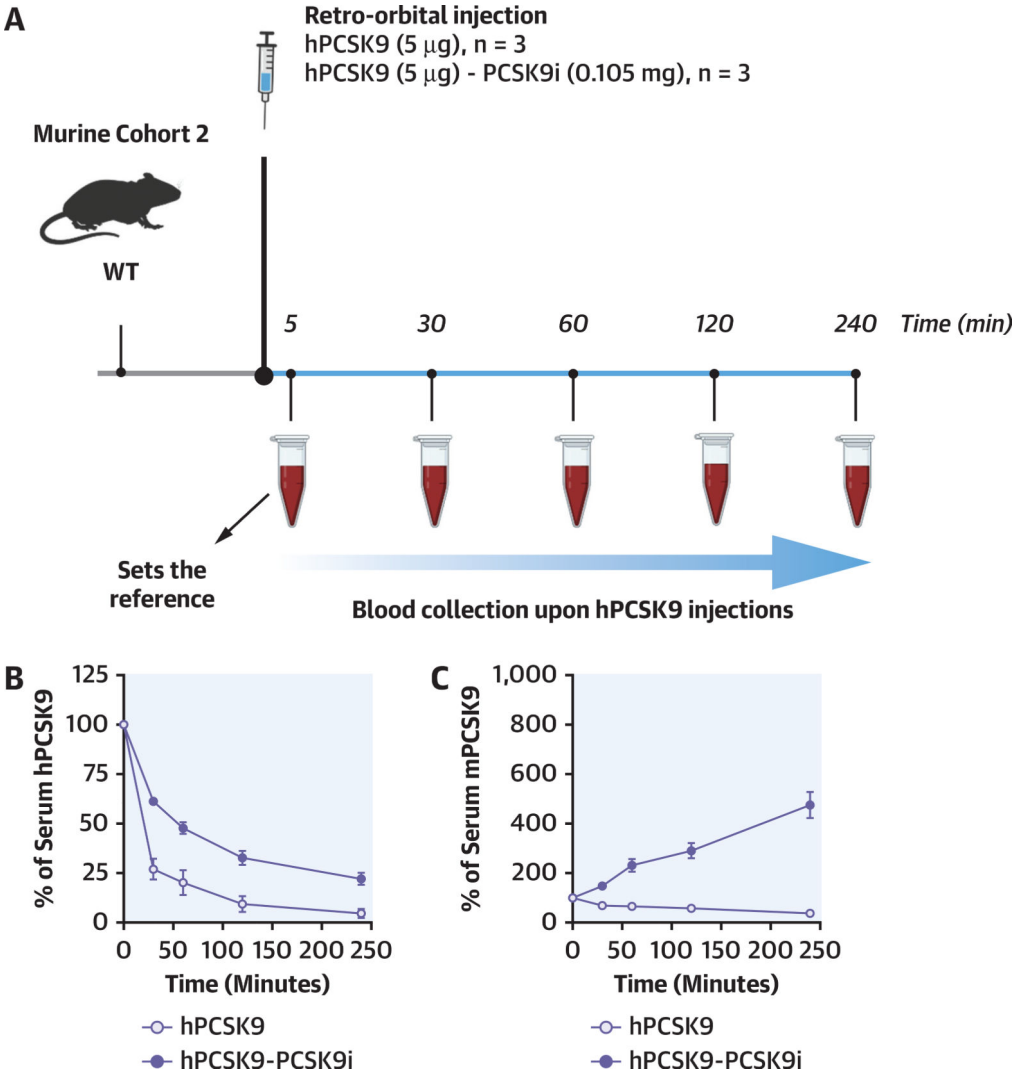

FIGURE 4. Effect of PCSK9i on PCSK9 Clearance

The clearance of free PCSK9 was compared with PCSK9 bound to PCSK9i. 5 μg of human PCSK9, either alone (n = 3) or after preincubation with 0.105 mg anti-PCSK9 antibody (n = 3) was administered to WT mice via retro-orbital injection. Blood samples were collected 5, 30, 60, 120, and 240 minutes after injection **(A)**. Human PCSK9 plasma levels were quantified and plotted relative to baseline **(B)**. Murine PCSK9 plasma levels were quantified and plotted relative to baseline **(C)**. Values are plotted as the mean ± SE, n = 3. Changes in circulating PCSK9 overtime and bound or not to the antibody were assessed for significance by 2-way analysis of variance (**B**: $P < 0.01$; **C**: $P < 0.001$). hPCSK9 = human PCSK9; mPCSK9 = murine PCSK9; other abbreviations as in Figures 1 and 3.

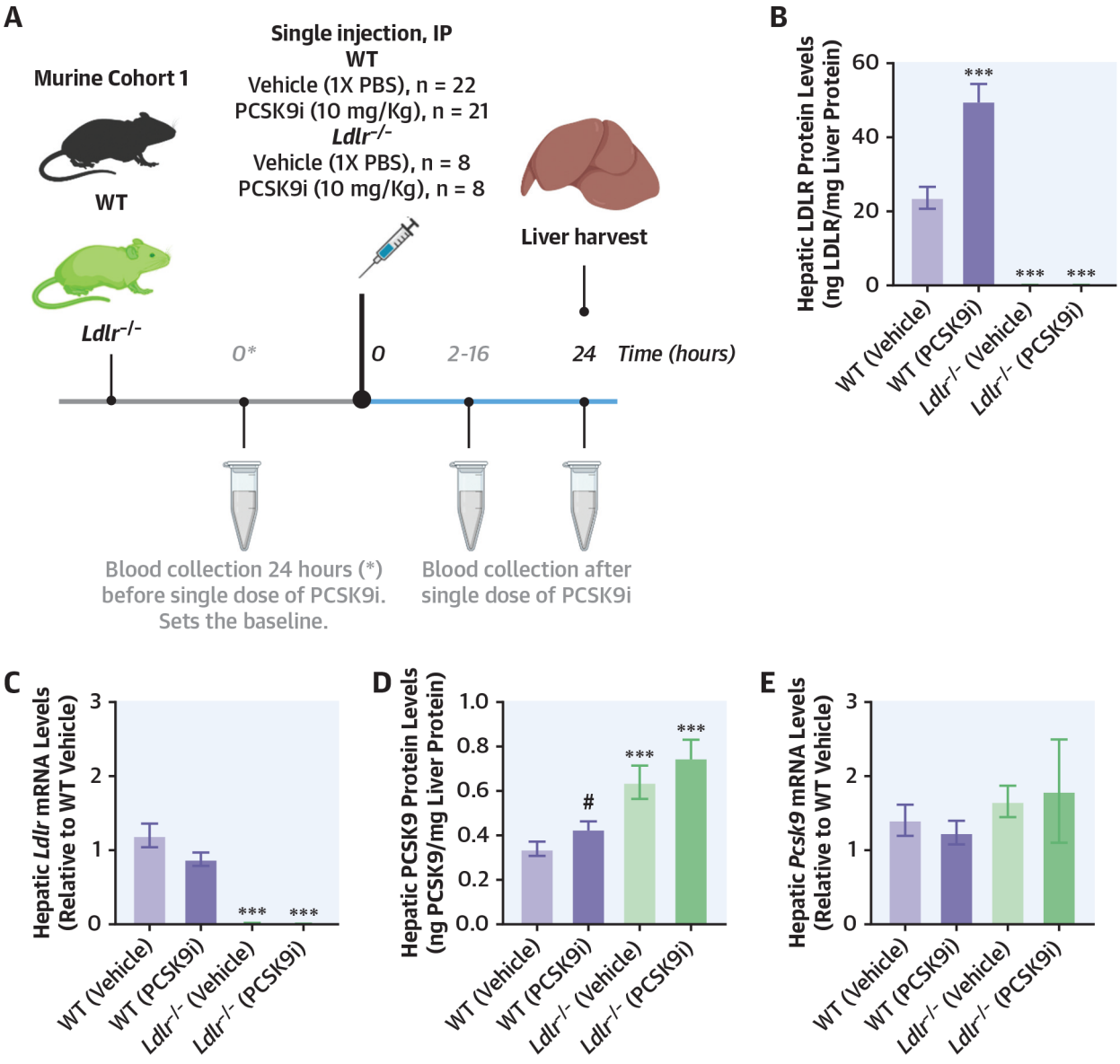

FIGURE 5. Short-Term Effects of PCSK9i in Murine Livers

WT and *Ldlr* $^{-/-}$ mice were given a single peritoneal injection of PCSK9i antibody (10 mg/kg) or vehicle (PBS). Livers were collected 24 hours after injection **(A)**. The effects of the antibody on hepatic LDLR protein **(B),** mRNA **(C)**, PCSK9 protein **(D)**, and mRNA **(E)** were quantified. Values are plotted as the mean ± SE (mRNA expression is relative to the WT control), n = 6–22. Changes were evaluated for significance by 2-tailed unpaired Student's *t*-test. #$P < 0.08$; ***$P < 0.001$. Abbreviations as in Figures 1 and 3.

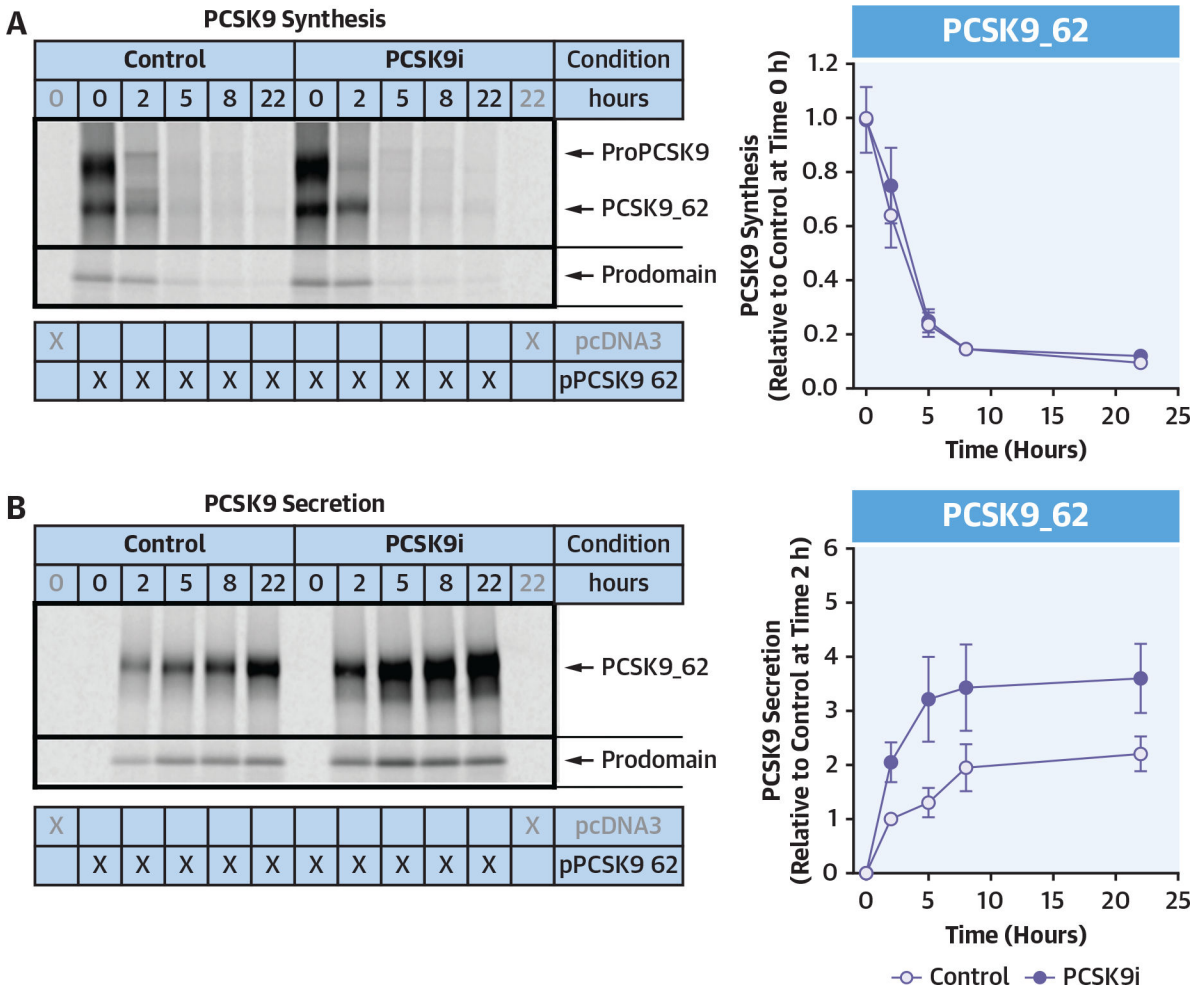

FIGURE 6. Kinetics of PCSK9 Production and Secretion In Vitro

Storage phosphor screen scans show the appearance and accumulation of PCSK9 over time in cell extracts **(A)** and media **(B)** from cells incubated with vehicle (1× PBS) or PCSK9i (PCSK9i, 8 μg/mL). Values are plotted as the mean ± SE (n = 4 independent experiments with 1 replicate in each experiment) of the quantified and normalized band intensity compared with control at time 0 or 2 hours. Changes in PCSK9, with or without antibody, were assessed for significance by 2-way analysis of variance (**B**: $P < 0.05$). Abbreviations as in Figure 1 and 3.

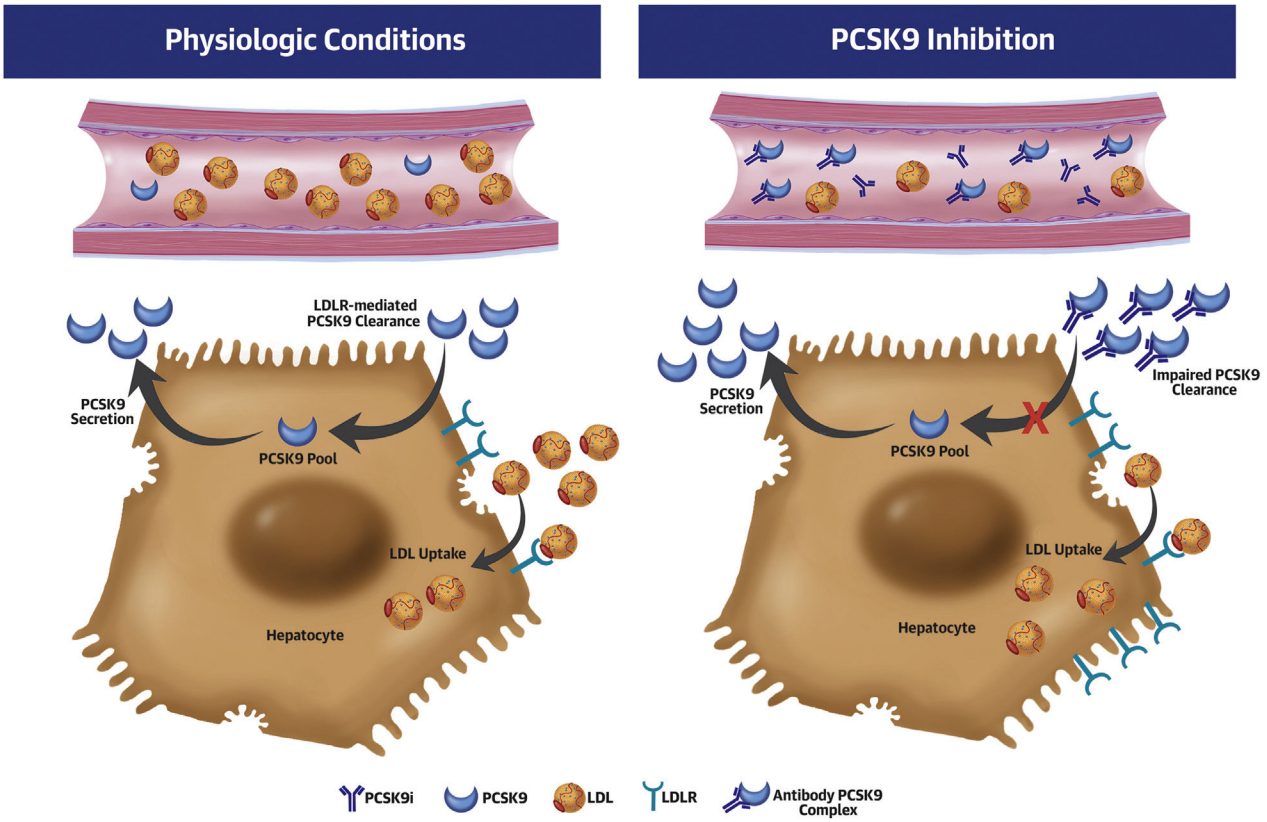

CENTRAL ILLUSTRATION. A Sensing Loop Regulates PCSK9 Secretion Upon Inhibitory Therapy

Two mechanisms contribute to the rapid increase in plasma PCSK9 levels in response to PCSK9 inhibition: the expected delayed clearance of the antibody-bound PCSK9; and an unexpected post-translational increase in PCSK9 secretion. Our results uncover a sensing loop for PCSK9 returning to the liver via low-density lipoprotein receptors and suggest that hepatic re-entry of plasma PCSK9 is a central contributor to trafficking of both PCSK9 and low-density lipoprotein. LDL= low-density lipoprotein; LDLR = low-density lipoprotein receptor; PCSK9 = proprotein convertase subtilisin/kexin type 9.

TABLE 1

Human Cohort 1 Patient Characteristics (n = 172)

Age, y	63 ± 11
Women	85 (49)
BMI, kg/m^2	29 ± 6
FH	73 (42)
Mild or heterozygous FH	71 (41)
Severe or homozygous FH	2 (1)
Plasma profile at baseline (before PCSK9i therapy)	
PCSK9, ng/mL	400 ± 173
Total cholesterol, mg/dL	223 ± 65
LDL-C, mg/dL	137 ± 57
HDL-C, mg/dL	54 ± 20
VLDL-C, mg/dL	36 ± 26
Triglycerides, mg/dL	182 ± 110
Medications	
Statins	86 (50)
Ezetimibe	118 (69)
Niacin	3 (2)
Fibrate	4 (2)
Bile acid sequestrant	3 (2)
Omega 3 fatty acids	29 (17)
PCSK9i therapy	
Alirocumab (75 mg every 2 weeks)	59 (34)
Evolocumab (140 mg every 2 weeks)	113 (66)

Values are mean ± SD or n (%).

BMI = body mass index; FH = familial hypercholesterolemia; HDL-C = high-density lipoprotein cholesterol; LDL-C = low-density lipoprotein cholesterol; PCSK9i = proprotein convertase subtilisin/kexin type 9 inhibitory therapy with monoclonal antibodies; VLDL-C = very low-density lipoprotein cholesterol.

TABLE 2

Human Cohort 2 Participant Characteristics (n = 7)

Age, y (at start of study)	36 ± 6
Female	3 (43)
BMI, kg/m^2	23 ± 3
Plasma profile at baseline (before PCSK9i therapy)	
PCSK9, ng/mL	214 ± 121
Total cholesterol, mg/dL	184 ± 45
LDL-C, mg/dL	104 ± 31
HDL-C, mg/dL	65 ± 18
Triglycerides, mg/dL	71 ± 19
PCSK9i single injection	
Alirocumab (75 mg)	3
Evolocumab (140 mg)	4

Values are mean ± SD, n (%), or n.

Abbreviations as in Table 1.